Article

The Effect of Functional Group Polarity in Palladium Immobilized Multiwalled Carbon Nanotube Catalysis: Application in Carbon–Carbon Coupling Reaction

Boggarapu Praphulla Chandra [1,2], Zheqiong Wu [3], Susana Addo Ntim [3], Golakoti Nageswara Rao [1] and Somenath Mitra [3,*]

[1] Department of Chemistry, Sri Sathya Sai Institute of Higher Learning, Prasanthi Nilayam 515134, India; bpc2sai@gmail.com (B.P.C.); nageswar.rao@rediffmail.com (G.N.R.)

[2] School of Science, Technology, Engineering and Mathematics, University of Washington Bothell, Bothell, WA 98011, USA

[3] Department of Chemistry and Environmental Science, New Jersey Institute of Technology, Newark, NJ 07102, USA; zw52@njit.edu (Z.W.); sa57@njit.edu (S.A.N.)

[*] Correspondence: somenath.mitra@njit.edu; Tel.: +1-973-596-5611; Fax: +1-973-596-3586

check for updates

Abstract: Carbon nanotubes (CNTs) are effective supports for nanometals and together they represent hybrids that combine the unique properties of both. A microwave-induced reaction was used to deposit nanopalladium on carboxylated and octadecylamine functionalized multiwall CNTs, which were used to carry out C–C coupling reactions in dimethylformamide (DMF) and toluene. These hybrids showed excellent catalytic activity with yield as high as 99.8%, while its enhancement with respect to commercially available Pd/C catalyst reached as high as 109%, and the reaction times were significantly lower. The polarity of the functionalized form was found to be a significant factor with the polar carboxylated CNT showing better activity in DMF while the relatively nonpolar octadecyl amine was better in toluene. The results suggest the possibility of tailor making functionalized CNTs when used as catalyst supports.

Keywords: Pd-CNT nanohybrids; functionalized CNTs; polarity; semi-homogeneous catalysis; heck reaction

1. Introduction

Hybrid structures involving carbon nanotubes (CNTs) and metal nanoparticles (NM) combine the unique properties of both [1]. These have been used in gas and liquid phase catalysis as well as electro catalysis [2–14]. Several CNT-NM hybrids have shown excellent reactivity [15–23], and different synthetic procedures have been used to immobilize Pt, Pd, Ru, and Rh NPs and a Rh/Pd alloy on CNTs. Various approaches [8–14] have been used to attach noble metals to CNTs [24–27]. These include in situ reduction [10], covalent bonding, electrostatic deposition, and physisorption [28]. Direct chemical reduction has been shown to increase metal loadings by as much as 50-fold [29] and microwave reactions have been reported as a fast method [30–33].

The pd-catalyzed reaction between aryl or alkenyl halides and olefins to deliver substituted olefins with high E-selectivity—known as the Heck reaction—is one of the most fundamental reactions in cross-coupling chemistry [34,35]. Initially, soluble Pd/Pt containing organometallic compounds were used as catalysts [34,35]. Later on, metal nanoparticle coated CNTs which represents the next generation of homogeneous catalyst were used to carry out these cross-coupling reactions. These have an advantage of easy separation of catalyst through centrifugation or precipitation [34–36].

In these typical reactions, the particle size, surface area, dispersion, and chemical nature of the support are important parameters [37–39]. In the case of CNT-NM, the presence of functional groups can alter many of these properties, but its role is not well understood. An added advantage of CNTs is that covalently introducing functional groups such as carboxylic carboxylic (–COOH), and (–CONH$_2$) can make them dispersible in different solvents and can be made solvent dispersible for different liquid phase reactions [40–42]. The synthesis of highly dispersed CNT-NM hybrids has been a challenge and is highly desirable for liquid phase reactions. We have reported the microwave induced synthesis CNT-Pt for catalytic hydrogenation of m-nitrochlorobenzene [19]. The objective of this work is to study the effect of CNT functionalization in CNT-Pd hybrids as applied to the Heck reaction and to study the effect of parameters such as dispersibility and polarity.

2. Experimental Section

2.1. Materials and Methods

Multiwall carbon nanotubes (MWCNT) (OD 20–30 nm, Purity 95%) were purchased from Cheap Tubes Inc. (Cambridgeport, VT, USA), and all other chemicals (iodobenzene, styrene, triphenylphosphine, (5 wt % Pd/C and PdCl$_2$)) were purchased from Sigma Aldrich (Bengaluru, Karnataka, India) with purity higher than 95%.

2.2. Synthesis of CNT-Metal Nanohybrids

Carboxylated Multiwall Carbon Nanotubes (MWCNT-COOH) were synthesized following a previously published methodology [42]. Briefly, the CNTs were functionalized in a Microwave Accelerated Reaction System (Mode: CEM Mars, CEM Corporation, 3100 Smith Farm Road, Matthews, NC, USA) fitted with internal temperature and pressure controls. Pre-weighed amounts of purified MWCNT were treated with a mixture of concentrated H$_2$SO$_4$ and HNO$_3$ solution under microwave radiation at 140 °C for 20 min. This led to the formation of carboxylic groups on the surface leading to high aqueous dispersibility. The resulting solid was filtered through a 10 μm membrane filter, washed with water to a neutral pH and dried under vacuum at 80 °C to a constant weight.

The MWCNT-COOH was used as the starting material to synthesize organic dispersible MWCNTs [43]. Pre-weighed amounts of MWCNT-COOH were mixed with thionylchloride (SOCl$_2$) and dimethylformamide (DMF) and were subjected to microwave radiation at 70 °C for 20 min leading to formation of MWCNT-COCl. The product was filtered and washed with THF till and was then dried in a vacuum oven at room temperature for 12 h. MWCNT-COCl was then reacted with octadecylamine (ODA) under microwave radiation at 120 °C for 10 min. The product was filtered and washed with hot ethanol and dichloromethane and dried at room temperature under vacuum to obtain MWCNT-ODA. The products MWCNT-COOH and MWCNT-ODA were used to synthesize the palladium loaded functionalized CNT nanohybrids: p-MWCNT-Pd and np-MWCNT-Pd respectively. The former was expected to be more polar. The p-MWCNT-Pd and np-MWCNT-Pd were synthesized by direct chemical reduction of metal salts as previously published by our group [19]. Pre-weighed amounts of the selected CNTs (MWCNT-COOH or MWCNT-ODA) were added to the reaction chamber together with a palladium dichloride (PdCl$_2$)-ethanol mixture. The reactions were carried out under microwave radiation at 190 °C for 10 min. After cooling, the products were filtered, washed with 0.5 N hydrochloric acid and MilliQ water to a neutral pH. The products (p-MWCNT-Pd or np-MWCNT-Pd) were dried at room temperature in a vacuum oven to constant weight.

The CNT-NM hybrids were characterized using a scanning electron microscope (SEM, Zeiss, Oberkochen, Germany) fitted with an Energy Dispersive X-ray spectrometer (EDX, Zeiss, Oberkochen, Germany), Thermogravimetric analysis (TGA, Perkin Elmer Inc., Waltham, MA, USA), and Fourier Transform Infrared spectroscopy (FTIR, Perkin Elmer Inc., Waltham, MA, USA). SEM data was collected on a LEO 1530 VP Scanning Electron Microscope equipped with an energy-dispersive X-ray analyzer. TGA was performed using a Pyris 1 TGA (Perkin-Elmer Inc., Waltham, MA, USA). FTIR measurements

were carried out in purified Pottasium bromide (KBr) pellets using a Perkin-Elmer (Spectrum One) instrument (Perkin Elmer Inc., Waltham, MA, USA).

2.3. Catalytic C–C Coupling

Heck reaction was carried out as follows. CNT-NM (p-MWCNT-Pd or np-MWCNT-Pd) (3 mg, 0.01 mol %), iodobenzene (496.8 μL, 4.44 mmol), styrene (765.1 μL, 6.69 mmol), tributylamine (TBA) (2.014 mL, 8.92 mmol) and 0.5 mg PPh$_3$ were mixed in 5 mL of dry solvent in a two necked round bottom flask. The resulting suspension was placed in a preheated rota-mantle at 140 °C with magnetic stirring. The course of the reaction was followed by periodically withdrawing aliquots (50 μL) from the reaction mixture and analyzing by GC. The reaction was carried out with triphenylphosphine (PPh$_3$) in dimethylformamide (DMF) and toluene. The same reaction was carried out with commercial Pd/C (24 mg, 0.01 mol %) and also with PdCl$_2$ (2 mg, 0.01 mol %) to compare the catalytic activity of the CNT-NMs. The reaction is shown in Scheme 1.
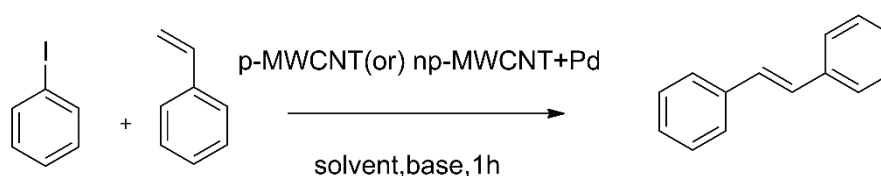
Scheme 1. General representation of reaction.

After 1 h reflux, the mixture was cooled for 15 min and extracted with diethyl ether. This was followed by washing with 2 N HCl and water to remove any base present. The ether layer was then dried over CaCl$_2$. Finally, the solution was filtered and dried in vacuum desiccator to constant weight. The obtained product was recrystallized from absolute alcohol and its composition was confirmed by comparison with pure stilbene. The final product did not show the presence of any byproducts by thin layer chromatography (TLC) analysis. The melting point of the recrystallized product and UV-λ_{max} were found to be 122.5 °C and 296 nm which was in line with what was expected for pure stilbene [44]. GC analysis of the product also showed only the presence of stilbene.

The aforementioned reactions were also carried out in microwave conditions at 420 W [45]. The amount of reactant, catalyst, and base (but no solvent) were maintained the same as done under reflux conditions. But, here the vessel was kept in microwave oven for 17 min where reaction went to completion with no reactant observed in the TLC analysis.

3. Results and Discussion

3.1. Nanohybrid Characterization

Figure 1 shows the SEM images of MWCNT-COOH, p-MWCNT-Pd, np-MWCNT-Pd and Pd/C. The MWCNTs had diameter in the range of 20–40 nm and the length was about 10–30 μm. There was no detectable change in tube morphology after acid treatment or after hybrid formation, implying that there was minimal visible damage to the tube structure. It is quite evident from the SEM images that the CNTs were coated with the metal nanoparticles. The EDX data shows large amounts of metal particles on the surface of the CNTs which are around 41.02% and 36.78% for p-MWCNT-Pd and np-MWCNT-Pd, respectively. The size of Pd particles ranged from 1 to 10 nm on p-MWCNT-Pd and from 5 to 50 nm on np-MWCNT-Pd. This implied that the catalyst was nanostructured and this was expected to contribute towards enhanced activity [19].

The FTIR spectra shown in Figure 2 confirmed the presence of functional groups in MWCNT-COOH, MWCNT-ODA, p-MWCNT-Pd, and np-MWCNT-Pd hybrids. The carbonyl stretching frequency in MWCNT-COOH was seen at 1716 cm^{-1} (COOH). The 3440 cm^{-1} band (O–H) present in MWCNT-COOH spectrum was attributed to the hydroxyl vibration of the carboxylic acid

group introduced through functionalization. In Figure 2b, the peaks around 1636 cm^{-1} and 1715 cm^{-1} were attributed to stretching vibrations of the amide C=O group, the sharp peaks at 2921 cm^{-1} and 2847 cm^{-1} were attributed to the C–H stretching vibration of the alkyl chain from ODA, the peak at 3460 cm^{-1} was attributed to the N–H stretching vibration from ODA, and the peak at 1250 cm^{-1} was attributed to C–N stretching vibration. In all the samples, the peak around 1580 cm^{-1} was assigned to the C=C stretching of the carbon skeleton. The appearance of new bands at 993 cm^{-1} and 996 cm^{-1} in the spectra for the hybrids confirmed the presence of Pd [37–39]. The broad peak centered around 3440 cm^{-1} in MWCNT-COOH was not prominent in the IR spectrum of p-MWCNT-Pd, and the shift in the carbonyl stretching frequency from 1716 cm^{-1} to 1721 cm^{-1} in the spectra for the hybrids indicated interaction of Pd with the COOH group.
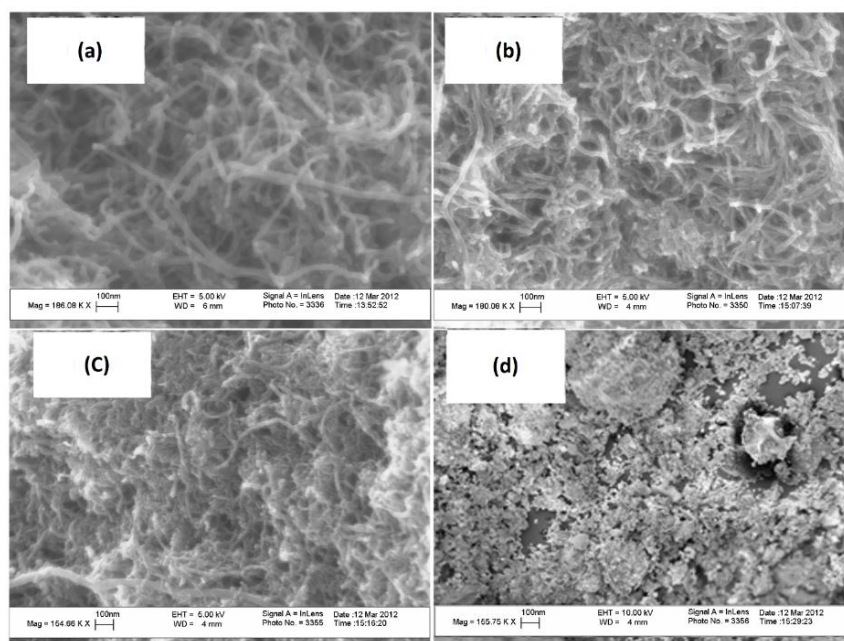

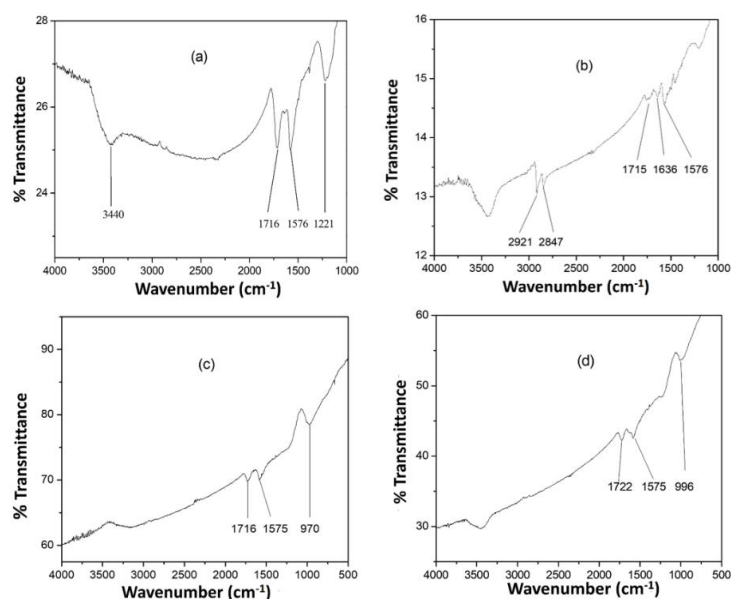**Figure 1.** SEM images of (**a**) MWCNT-COOH, (**b**) p-MWCNT-Pd, (**c**) np-MWCNT-Pd, and (**d**) Pd/C.

Figure 2. FTIR data for (**a**) MWCNT-COOH, (**b**) MWCNT-ODA, (**c**) p-MWCNT-Pd, and (**d**) np-MWCNT-Pd.

3.2. Dispersibility

Figure 3a–f shows the dispersibility of p-MWCNT-Pd (5 mg), np-MWCNT-Pd (5 mg), and Pd/C (5 mg) in *N,N*-dimethylformamide (5 mL), and toluene (5 mL). It is evident that p-MWCNT-Pd, np-MWCNT-Pd, and Pd/C were significantly more dispersible in DMF than in toluene. The particle size of the dispersed CNT-NM is presented in Table 1. It shows that there is not much difference between p-MWCNT-Pd and np-MWCNT-Pd in toluene, but there was significant difference in DMF. The particle size of CNT-NM agglomerates in toluene were higher than those in DMF. As can be seen in Figure 3, there was significant precipitation of the MWCNT-Pd in toluene, so the particle size represents what remained dispersed. The colloidal dispersion in DMF and TBA remained homogeneously suspended for several weeks without need for mechanical stirring.
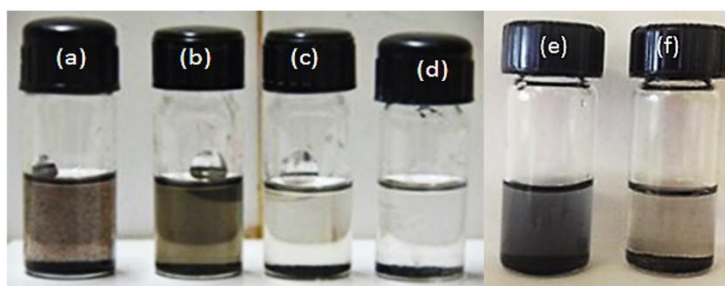

Figure 3. Photographs of different dispersions: (**a**) np-MWCNT-Pd dispersed in DMF, (**b**) p-MWCNT-Pd dispersed in DMF, (**c**) np-MWCNT-Pd in Toluene, (**d**) p-MWCNT-Pd in Toluene; (**e**) Pd/C dispersed in DMF, (**f**) Pd/C dispersed in Toluene.

Table 1. Particle size of dispersible CNT-NM.

Samples/Solvents	p-MWCNT-Pd	np-MWCNT-Pd
Toluene	240.3 nm	234.2 nm
Dimethylformamide (DMF)	168.2 nm	126.4 nm

The metal nanoparticles loading in the hybrid materials were quantified using TGA as shown in Figure 4. The resulting weight above 600 °C was attributed to the weight of residual metal. The nanohybrids were found to contain 43.02 and 38.93 percent by weight of Pd in p-MWCNT-Pd and np-MWCNT-Pd, respectively, while Pd/C contained 5% by weight of Pd.
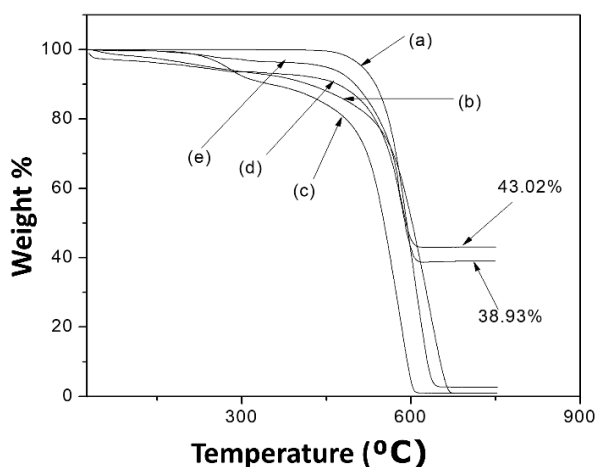

Figure 4. TGA of (**a**) MWCNT, (**b**) MWCNT-COOH, (**c**) MWCNT-ODA, (**d**) p-MWCNT-Pd, and (**e**) np-MWCNT-Pd.

3.3. Effect of CNT Functionalization

The CNT-NM hybrids were used as catalysts in the Heck reaction of iodobenzene with styrene. All the reactions were carried out keeping substrate to Pd molar ratio constant at 0.01 mole percent. In all cases, trans-stilbene was the only product detected which was established by the single spot in the TLC analysis and confirmed by GC analysis. This was also confirmed by the melting point of 122.5 °C and UV max at 296 nm of the isolated product.

The mechanism of the reaction in presence of PPh$_3$ is shown in Figure 5. In general, the Pd from the CNT-NM desorbed to a soluble form to form a loose complex such as Pd(PPh$_3$)$_4$. These complexes were more soluble than Pd and facilitated desorption of Pd from the catalyst. This may account for the high yield observed in the presence of PPh$_3$. At the end of the reaction, the Pd readsorbed on the CNT phase.
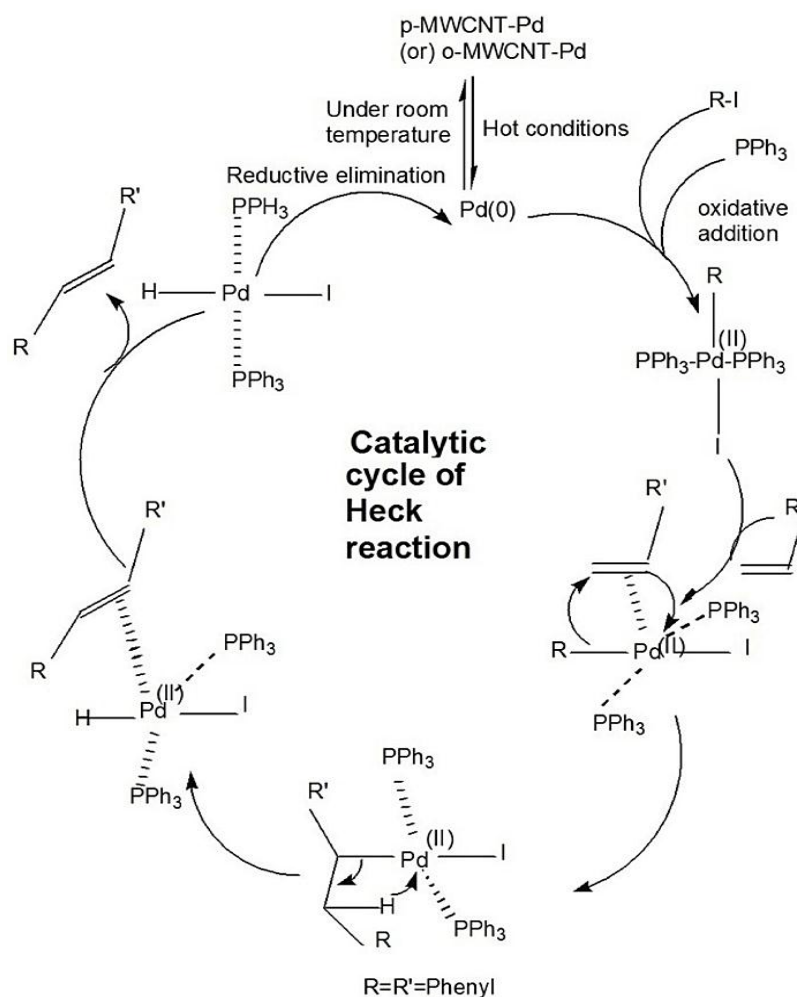

Figure 5. The role of CNT-Pd in the in the Heck reaction.

Table 2 presents isolated yields of all the reactions after the completion of the reaction and recrystallization. The results of reaction at 150 °C are presented in Table 2 and Figure 6. In general, shorter reaction times and greater yields were obtained with p-MWCNT-Pd and np-MWCNT-Pd compared to Pd/C, demonstrating the superiority of these nanohybrids in the reaction. The time to completion for the reaction for both p-MWCNT-Pd and np-MWCNT-Pd were 60 min in DMF compared to 90 min for Pd/C. Similar results are also seen in Figure 6, where yield enhancement of CNT-NM hybrids with respect to Pd/C is also presented.

Table 2.　**Table 2.**　Isolated yields of all the reactions at completion.　Analysis was done after recrystallization.

S.No.	Catalyst	Reaction Completion Time (min)	% Yield	Yield Enhancement
Dimethylformamide (DMF) as solvent				
1	Pd/C	90	55.70	-
2	np-MWCNT-Pd	60	58.70	5%
3	p-MWCNT-Pd	60	99.78	79%
4	PdCl$_2$	120	45.67	-
Toluene as solvent				
5	Pd/C	105	10.90	-
6	p-MWCNT-Pd	90	14.39	32%
7	np-MWCNT-Pd	90	17.44	60%
Microwave (solvent free)				
8	p-MWCNT-Pd	17	90.01	-
9	np-MWCNT-Pd	17	66.92	-
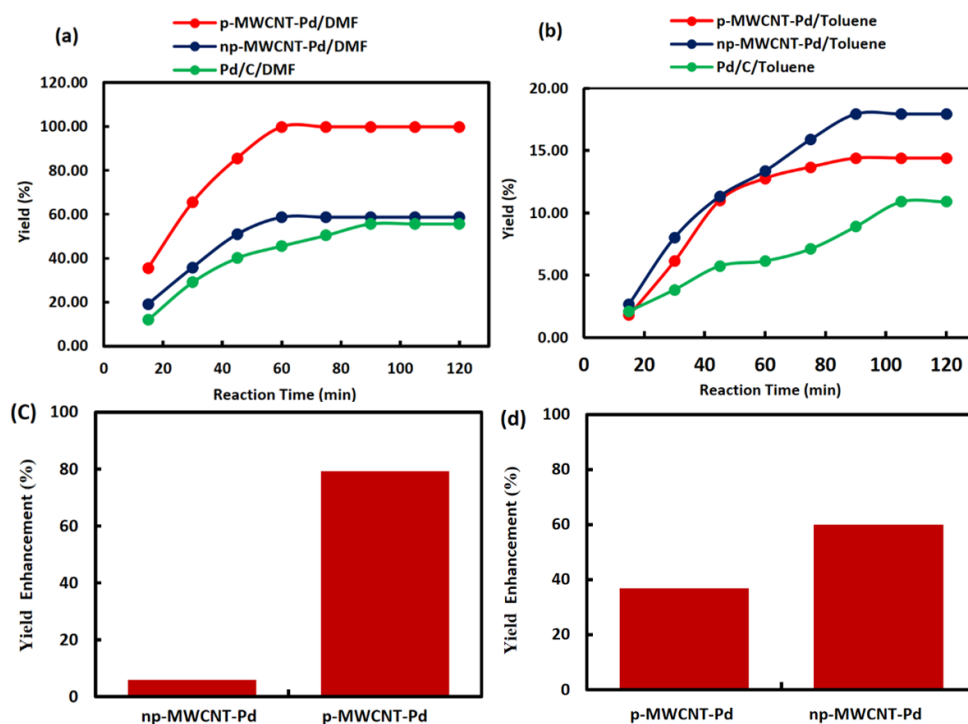
Figure 6. Yields of the CNT-metal nanohybrids and Pd/C catalyzed reactions (**a**) in DMF and (**b**) in toluene from GC analysis (Tri-butyl amine as base, temp 150 °C); (**c**) yield enhancement with respect to Pd/C in DMF; (**d**) enhancement with respect to Pd/C in toluene.

It is estimated that the ODA group will cause steric hindrance of the reactants. To test this hypothesis, the reactions were carried out under microwave conditions in absence of solvent. The reaction was complete in 17 min. During microwave heating, the CNT catalysts were seen to mix uniformly in the reaction mixture. The isolated yields for the reactions are shown in Table 2. The yield was much higher in the p-MWCNT-Pd than in np-MWCNT-Pd. The difference was attributed to steric effects, where the ODA group provided steric hindrances leading to lower yield.

In DMF, the p-MWCNT-Pd showed higher catalytic activity than np-MWCNT-Pd which was better than commercial Pd/C and PdCl$_2$. The yield for p-MWCNT-Pd reached as high as 99.78% in DMF,

whereas np-MWCNT-Pd, Pd/C, and PdCl$_2$ showed yields of 58.7%, 55.7%, and 45.7%, respectively. The catalytic activity of p-MWCNT-Pd with larger particle size was higher than np-MWCNT-Pd with smaller particle size (Table 1). The p-MWCNT-Pd was more polar than np-MWCNT-Pd and its interactions with DMF, which is a polar solvent, were better. Also, the long C$_{18}$ chain from octadecyl group in np-MWCNT-Pd may have provided some steric hindrance to the reactants. Thus, the polarity and functionalized forms of support material are important in the matter of catalytic activity.

In the case of toluene as solvent, the results were the opposite. The np-MWCNT-Pd showed significantly higher catalytic activity than p-MWCNT-Pd, which was better than Pd/C. Compared to Pd/C, the enhancement for np-MWCNT-Pd and p-MWCNT-Pd were 60% and 32% respectively. Therefore, the enhancement nearly doubled for the nonpolar np-MWCNT-Pd. In this case, the catalytic activity of p-MWCNT-Pd with larger particle size was lower than np-MWCNT-Pd with smaller particle size. The steric hindrance from the octadecyl group did not reduce yield. Therefore, the higher yield of np-MWCNT-Pd was attributed to the higher interactions of the nonpolar np-MWCNT-Pd with nonpolar toluene. Figure 6a,b show yield as a function of time in DMF and toluene, respectively. As already mentioned, DMF was the better solvent with these catalysts, with yield reaching as high as 99.78% in 60 min. Yields were relatively lower and reaction times were longer in toluene, which was in line with what has been reported before [34,35]. In the case of DMF, the reactions were completed in 60 min with the nanohybrids and it took 90 min with Pd/C. On the other hand, when toluene was the solvent, the time taken for the same reactions were 90 min with the nanohybrids, and 105 min with Pd/C. Yield enhancement of CNT-NM hybrids with respect to Pd/C for the Heck reaction at 60 min reaction time in both DMF and toluene are shown in Figure 6c,d. In DMF, the enhancements were 79% and 5% for p-MWCN-Pd and np-MWCN-Pd, respectively, while the corresponding enhancements in toluene were 32% and 60% in toluene. It is evident that the polarities of the functionalized form of catalysts and solvents is the important factor for catalytic activity. DMF is a better solvent than toluene for Heck reaction due to the greater dispersibility of the catalyst in DMF and high boiling point. High boiling point of the solvent enables the reaction to be carried out at a relatively higher temperature. Also, for catalysts containing polar groups (–COOH in this case), a polar aprotic solvent like DMF is a suitable solvent for Heck reaction.

The reason for higher yields in DMF compared to the toluene (Boiling Point (B.P); 110.6 °C) is due to the better dispersibility of catalyst in addition to the higher boiling point of DMF (B.P; 153 °C). Nevertheless, when toluene was used as the solvent, np-MWCNT-Pd showed significantly higher catalytic activity than p-MWCNT-Pd, which was better than Pd/C. These were also attributed to dispersibility of catalyst (refer to Figure 6). Hence, it is evident that disparities in the polarity play an important role.

3.4. Active Metal Requirement and Reusability

Since DMF was the better solvent, the catalyst requirement for CNT-NM was calculated. Typical Heck reaction with conventional palladium salts requires 1–2 mol % catalyst [34,35]. In the present work with MWCNT-Pd hybrids, significantly lower quantities of Pd (order of 0.01 mol % Pd) resulted in higher yield at shorter reaction times. Therefore, this study showed that nan palladium on functionalized CNTs is more effective than conventional palladium salts. The turnover frequency (TOF) of the two catalysts were calculated as follows:

$$\text{TOF} = \frac{\text{Product (mol)}}{\text{Pd (mol)} \times \text{Reaction time (h)}} \tag{1}$$

Under reflux conditions, the TOF of p-MWCNT-Pd and np-MWCNT-Pd in DMF were 9977 and 5863, respectively, and in toluene 1090 and 977, respectively, which shows that the polar p-MWCNT-Pd in polar solvent has higher catalytic activity. Under microwave conditions, the TOF of p-MWCNT-Pd and o-MWCNT-Pd were 9000 and 6681, respectively.

An important issue has been the reusability of the catalyst. In the case of p-MWCNT-Pd and np-MWCNT-Pd, leaching of Pd from MWCNT support to hot DMF was demonstrated by carrying out a reaction under the aforementioned conditions and filtering the solid catalyst after 30 min while the mixture was still hot (around 150 °C). The filtrate was allowed to reflux in the absence of solid catalyst and yield from the reaction was determined. The yields were found to remain the same in the presence of the p-MWCNT-Pd as well as np-MWCNT-Pd. This demonstrated that Pd desorbed from the CNT support had remained suspended into the liquid phase in hot condition.

Irreversible leaching is a major consideration while dealing with solid catalysts due to depletion in the metal content and subsequent loss in activity. In another set of experiments in DMF with p-MWCNT-Pd and np-MWCNT-Pd, the recovered catalysts obtained by filtration after one hour reaction and subsequent cooling to room temperature were reused for a three consecutive reactions. The yield obtained with recovered catalysts in each step was within 2% of the previous step yield. This showed that there was no significant decrease in the catalytic activity of the recovered catalyst. This can be explained by "boomerang effect" [45–47] where catalyst which is dispersed into the bulk solution under the hot condition from the solid support redeposits under cold conditions. In order to study this, the reaction mixture (after 1-h reaction) was filtered in the hot condition to recover the catalyst. Similarly, the reaction mixture (after 1 h) was filtered after cooling to room temperature. The catalysts were analyzed for Pd content. The weight percent of Pd from the hot and cold conditions in the p-MWCNT-Pd were 11.9 and 22.9, respectively, as determined by EDX. This supported the existence of boomerang effect. In the future, poison testing will be conducted for these catalysts to understand the nature of catalysis which assist in designing next generation catalysts.

4. Conclusions

p-MWCNT-Pd and np-MWCNT-Pd were synthesized using a microwave induced reaction and they showed high catalytic activity compared to commercially available Pd/C. The CNT-Pd needed a smaller amount of active catalyst but led to faster reactions and higher yields. The best reaction conditions were found to be with DMF as solvent, TBA as base, and triphenylphosphine as ligand. While p-MWCNT-Pd showed better performance in polar DMF, np-MWCNT-Pd was more effective in toluene. Matching the polarity of CNT functionalization with that of the solvent is clearly an effective way to maximize yield.

References

1. Yu, W.; Tu, W.; Liu, H. Synthesis of nanoscale platinum colloids by microwave dielectric heating. *Langmuir* **1999**, *15*, 6–9. [CrossRef]
2. Gong, K.; Chakrabarti, S.; Dai, L. Electrochemistry at carbon nanotube electrodes: Is the nanotube tip more active than the sidewall? *Angew. Chem. Int. Ed.* **2008**, *47*, 5446–5450. [CrossRef] [PubMed]

3.　Ovejero, G.; Sotelo, J.; Rodríguez, A.; Díaz, C.; Sanz, R.; García, J. Platinum catalyst on multiwalled carbon nanotubes for the catalytic wet air oxidation of phenol. *Ind. Eng. Chem. Res.* **2007**, *46*, 6449–6455. [CrossRef]

4.　Yang, X.; Cao, Y.; Yu, H.; Huang, H.; Wang, H.; Peng, F. Unravelling the radical transition during the carbon-catalyzed oxidation of cyclohexane by in situ electron paramagnetic resonance in the liquid phase. *Catal. Sci. Technol.* **2017**, *7*, 4431–4436. [CrossRef]

5.　Iglesias, D.; Senokos, E.; Alemán, B.; Cabana, L.; Navío, C.; Marcilla, R.; Prato, M.; Vilatela, J.J.; Marchesan, S. Gas-phase functionalization of macroscopic carbon nanotube fiber assemblies: Reaction control, electrochemical properties, and use for flexible supercapacitors. *ACS Appl. Mater. Interfaces* **2018**, *10*, 5760–5770. [CrossRef] [PubMed]

6.　Su, D.S.; Wen, G.; Wu, S.; Peng, F.; Schlögl, R. Carbocatalysis in Liquid-Phase Reactions. *Angew. Chem. Int. Ed.* **2017**, *56*, 936–964. [CrossRef] [PubMed]

7.　Lamme, W.S.; Zečević, J.; de Jong, K.P. Influence of Metal Deposition and Activation Method on the Structure and Performance of Carbon Nanotube Supported Palladium Catalysts. *ChemCatChem* **2018**, *10*, 1552–1555. [CrossRef] [PubMed]

8.　Kong, B.-S.; Jung, D.-H.; Oh, S.-K.; Han, C.-S.; Jung, H.-T. Single-walled carbon nanotube gold nanohybrids: Application in highly effective transparent and conductive films. *J. Phys. Chem. C* **2007**, *111*, 8377–8382. [CrossRef]

9.　Kauffman, D.R.; Star, A. Chemically induced potential barriers at the carbon nanotube-metal nanoparticle interface. *Nano Lett.* **2007**, *7*, 1863–1868. [CrossRef] [PubMed]

10.　Hu, X.; Wang, T.; Qu, X.; Dong, S. In situ synthesis and characterization of multiwalled carbon nanotube/Au nanoparticle composite materials. *J. Phys. Chem. B* **2006**, *110*, 853–857. [CrossRef] [PubMed]

11.　Shi, Y.; Yang, R.; Yuet, P.K. Easy decoration of carbon nanotubes with well dispersed gold nanoparticles and the use of the material as an electrocatalyst. *Carbon* **2009**, *47*, 1146–1151. [CrossRef]

12.　Hou, X.; Wang, L.; Zhou, F.; Wang, F. High-density attachment of gold nanoparticles on functionalized multiwalled carbon nanotubes using ion exchange. *Carbon* **2009**, *47*, 1209–1213. [CrossRef]

13.　Tzitzios, V.; Georgakilas, V.; Oikonomou, E.; Karakassides, M.; Petridis, D. Synthesis and characterization of carbon nanotube/metal nanoparticle composites well dispersed in organic media. *Carbon* **2006**, *44*, 848–853. [CrossRef]

14.　Zhang, M.; Su, L.; Mao, L. Surfactant functionalization of carbon nanotubes (CNTs) for layer-by-layer assembling of CNT multi-layer films and fabrication of gold nanoparticle/CNT nanohybrid. *Carbon* **2006**, *44*, 276–283. [CrossRef]

15.　Yoon, B.; Wai, C.M. Microemulsion-Templated Synthesis of Carbon Nanotube-Supported Pd and Rh Nanoparticles for Catalytic Applications. *J. Am. Chem. Soc.* **2005**, *127*, 17174–17175. [CrossRef] [PubMed]

16.　Planeix, J.; Coustel, N.; Coq, B.; Brotons, V.; Kumbhar, P.; Dutartre, R.; Geneste, P.; Bernier, P.; Ajayan, P. Application of carbon nanotubes as supports in heterogeneous catalysis. *J. Am. Chem. Soc.* **1994**, *116*, 7935–7936. [CrossRef]

17.　Corma, A.; Garcia, H.; Leyva, A. Catalytic activity of palladium supported on single wall carbon nanotubes compared to palladium supported on activated carbon: Study of the Heck and Suzuki couplings, aerobic alcohol oxidation and selective hydrogenation. *J. Mol. Catal. A Chem.* **2005**, *230*, 97–105. [CrossRef]

18.　Guo, D.-J.; Li, H.-L. High dispersion and electrocatalytic properties of palladium nanoparticles on single-walled carbon nanotubes. *J. Colloid Interface Sci.* **2005**, *286*, 274–279. [CrossRef] [PubMed]

19.　Chen, Y.; Zhang, X.; Mitra, S. Solvent dispersible nanoplatinum-carbon nanotube hybrids for application in homogeneous catalysis. *Chem. Commun.* **2010**, *46*, 1652–1654. [CrossRef] [PubMed]

20.　Mu, Y.; Liang, H.; Hu, J.; Jiang, L.; Wan, L. Controllable Pt nanoparticle deposition on carbon nanotubes as an anode catalyst for direct methanol fuel cells. *J. Phys. Chem. B* **2005**, *109*, 22212–22216. [CrossRef] [PubMed]

21.　Zhang, K.; Zhang, F.J.; Chen, M.L.; Oh, W.C. Comparison of catalytic activities for photocatalytic and sonocatalytic degradation of methylene blue in present of anatase TiO_2–CNT catalysts. *Ultrason. Sonochem.* **2011**, *18*, 765–772. [CrossRef] [PubMed]

22.　Chandrasekhar, P. CNT Applications in Microelectronics, Nanoelectronics, and Nanobioelectronics. In *Conducting Polymers, Fundamentals and Applications*; Springer: Berlin, Germany, 2018; pp. 65–72.

23.　Karakoti, M. Surface Modification of Carbon-Based Nanomaterials for Polymer Nanocomposites. In *Carbon-Based Polymer Nanocomposites for Environmental and Energy Applications*; Ismail, A.F., Goh, P.S., Eds.; Elsevier: Amsterdam, The Netherlands, 2018; pp. 27–56.

24. Lordi, V.; Yao, N.; Wei, J. Method for supporting platinum on single-walled carbon nanotubes for a selective hydrogenation catalyst. *Chem. Mater.* **2001**, *13*, 733–737. [CrossRef]

25. Ellis, A.V.; Vijayamohanan, K.; Goswami, R.; Chakrapani, N.; Ramanathan, L.; Ajayan, P.M.; Ramanath, G. Hydrophobic anchoring of monolayer-protected gold nanoclusters to carbon nanotubes. *Nano Lett.* **2003**, *3*, 279–282. [CrossRef]

26. Giordano, R.; Serp, P.; Kalck, P.; Kihn, Y.; Schreiber, J.; Marhic, C.; Duvail, J.L. Preparation of rhodium catalysts supported on carbon nanotubes by a surface mediated organometallic reaction. *Eur. J. Inorg. Chem.* **2003**, *2003*, 610–617. [CrossRef]

27. Haremza, J.M.; Hahn, M.A.; Krauss, T.D.; Chen, S.; Calcines, J. Attachment of single CdSe nanocrystals to individual single-walled carbon nanotubes. *Nano Lett.* **2002**, *2*, 1253–1258. [CrossRef]

28. Azamian, B.R.; Coleman, K.S.; Davis, J.J.; Hanson, N.; Green, M.L. Directly observed covalent coupling of quantum dots to single-wall carbon nanotubes. *Chem. Commun.* **2002**, 366–367. [CrossRef]

29. Liu, Z.; Lin, X.; Lee, J.Y.; Zhang, W.; Han, M.; Gan, L.M. Preparation and characterization of platinum-based electrocatalysts on multiwalled carbon nanotubes for proton exchange membrane fuel cells. *Langmuir* **2002**, *18*, 4054–4060. [CrossRef]

30. Cano, M.; Benito, A.; Maser, W.K.; Urriolabeitia, E.P. One-step microwave synthesis of palladium–carbon nanotube hybrids with improved catalytic performance. *Carbon* **2011**, *49*, 652–658. [CrossRef]

31. Trusova, M.E.; Rodriguez-Zubiri, M.; Kutonova, K.V.; Jung, N.; Bräse, S.; Felpin, F.X.; Postnikov, P.S. Ultra-fast Suzuki and Heck reactions for the synthesis of styrenes and stilbenes using arenediazonium salts as super-electrophiles. *Org. Chem. Front.* **2018**, *5*, 41–45. [CrossRef]

32. Ichikawa, T.; Mizuno, M.; Ueda, S.; Ohneda, N.; Odajima, H.; Sawama, Y.; Monguchi, Y.; Sajiki, H. A practical method for heterogeneously-catalyzed Mizoroki–Heck reaction: Flow system with adjustment of microwave resonance as an energy source. *Tetrahedron* **2018**, *74*, 1810–1816. [CrossRef]

33. Díaz-Ortiz, Á.; Prieto, P.; Vázquez, E. Heck reactions under microwave irradiation in solvent-free conditions. *Synlett* **1997**, *3*, 269–270. [CrossRef]

34. Christoffel, F.; Ward, T.R. Palladium-catalyzed Heck cross-coupling reactions in water: A comprehensive review. *Catal. Lett.* **2018**, *148*, 489–511. [CrossRef]

35. Beletskaya, I.P.; Cheprakov, A.V. The Heck reaction as a sharpening stone of palladium catalysis. *Chem. Rev.* **2000**, *100*, 3009–3066. [CrossRef] [PubMed]

36. Yang, X.; Wang, X.; Qiu, J. Aerobic oxidation of alcohols over carbon nanotube-supported Ru catalysts assembled at the interfaces of emulsion droplets. *Appl. Catal. A* **2010**, *382*, 131–137. [CrossRef]

37. Daniel, M.-C.; Astruc, D. Gold nanoparticles: Assembly, supramolecular chemistry, quantum-size-related properties, and applications toward biology, catalysis, and nanotechnology. *Chem. Rev.* **2004**, *104*, 293–346. [CrossRef] [PubMed]

38. Moreno-Manas, M.; Pleixats, R. Formation of carbon-carbon bonds under catalysis by transition-metal nanoparticles. *Acc. Chem. Res.* **2003**, *36*, 638–643. [CrossRef] [PubMed]

39. Corain, B.; Kralik, M. Generating palladium nanoclusters inside functional cross-linked polymer frameworks. *J. Mol. Catal. A Chem.* **2001**, *173*, 99–115. [CrossRef]

40. Li, W.; Liang, C.; Qiu, J.; Zhou, W.; Han, H.; Wei, Z.; Sun, G.; Xin, Q. Carbon nanotubes as support for cathode catalyst of a direct methanol fuel cell. *Carbon* **2002**, *40*, 791–794. [CrossRef]

41. Li, W.; Liang, C.; Zhou, W.; Qiu, J.; Zhou, Z.; Sun, G.; Xin, Q. Preparation and characterization of multiwalled carbon nanotube-supported platinum for cathode catalysts of direct methanol fuel cells. *J. Phys. Chem. B* **2003**, *107*, 6292–6299. [CrossRef]

42. Chen, Y.; Mitra, S. Fast Microwave-Assisted Purification, Functionalization and Dispersion of Multi-Walled Carbon Nanotubes. *J. Nanosci. Nanotechnol.* **2008**, *8*, 5770–5775. [CrossRef] [PubMed]

43. Desai, C.; Addo Ntim, S.; Mitra, S. Antisolvent precipitation of hydrophobic functionalized multiwall carbon nanotubes in an aqueous environment. *J. Colloid Interface Sci.* **2012**, *368*, 115–120. [CrossRef] [PubMed]

44. Wheeler, O.H.; Pabon, H.N.B. Synthesis of Stilbenes. A Comparative Study1. *J. Org. Chem.* **1965**, *30*, 1473–1477. [CrossRef]

45. Sermon, P.; Bond, G. Hydrogen spillover. *Catal. Rev.* **1974**, *8*, 211–239. [CrossRef]

46. Sun, W.; Liu, Z.; Jiang, C.; Xue, Y.; Chu, W.; Zhao, X. Experimental and theoretical investigation on the interaction between palladium nanoparticles and functionalized carbon nanotubes for Heck synthesis. *Catal. Today* **2013**, *212*, 206–214. [CrossRef]

47. Bond, G.C. A Short History of Hydrogen Spillover. In *Studies in Surface Science and Catalysis*; Pajonk, G.M.S.J.T., Germain, J.E., Eds.; Elsevier: Amsterdam, The Netherlands, 1983; pp. 1–16.